ELSEVIER

Journal of Hazardous Materials 38 (1994) 13–25

JOURNAL OF HAZARDOUS MATERIALS

An enhanced adiabatic calorimeter for thermal hazard analysis

Ming-Huei Yue

Process Safety Laboratory, Merck & Co., Inc., One Merck Drive, P.O. Box 100, WS-EX, Whitehouse Station, NJ 08889, USA

Accepted in revised form 29 September 1993

Abstract

An enhanced adiabatic calorimeter (EAC) has been developed to study thermal runaway reactions under adiabatic conditions and to generate data for applying DIERS Technology [1]. Similar in concept to the Union Carbide's APTAC device [2], EAC operates with a ϕ factor close to 1.05, and achieves an exotherm detection sensitivity of $\approx 0.02\,^{\circ}C/min$. Other desirable features, such as remote feed capability and a quench vessel, were also incorporated. Characterization of EAC has been conducted by using both inert and reactive chemicals. Inert samples were used to determine the long-term drift rate and the effect of calibration uncertainty on exotherm detection sensitivity. The well-known thermal decomposition of di-tert-butyl peroxide (DTBP) was used as a sample reactive system.

1. Introduction

Safety has been one of the major concerns in the chemical process industry, particularly over the past few decades. Several adiabatic instruments, including the Accelerating Rate Calorimeter (ARC™) [3, 4] and Vent Sizing Package (VSP™) [1, 5, 6], have evolved as key testing apparatuses to determine if a process stream has the potential to runaway and cause explosions. Data obtained from ARC, VSP, and/or other adiabatic devices are commonly used to estimate the heat of a runaway reaction, the time to maximum reaction rate, the kinetic parameters and the detected reaction onset temperature, which is frequently referred as the exotherm initiation temperature. Based on these and other process-related information, the emergency relief venting requirements can then be determined by applying DIERS Technology, and an emergency response plan to mitigate runaway hazards can also be devised.

ARC and VSP usually compliment each other in obtaining a more thorough profile of runaway reactions. ARC [3] has an excellent exotherm detection sensitivity of 0.02 °C/min and, as a result, can detect the presence of exothermic

0304-3894/94/$07.00
SSDI 0304-3894(93)E0091-F

reactions at relatively low temperatures. However, ARC test cells are relatively heavy compared to the sample weight; therefore, heat absorbed by the test cell during an exotherm is much larger than that normally experienced in process vessels. A dimensionless quantity called the ϕ factor [5] or thermal inertia is typically used to characterize this effect:

$$\phi = 1 + m_b C_{vb}/m_s C_{vs},$$

where m_b and m_s are the masses of the test cell and the sample, respectively, and C_{vb} and C_{vs} are the average heat capacities of the test cell and sample, respectively. In typical ARC runs, the ϕ factor ranges from ≈ 1.5 to > 4, which is significantly larger than ~ 1.05 for typical process vessels after the initial stage of runaway reactions. As a result, testing conducted with ϕ factor close to 1 is usually recommended to confirm the kinetics derived from ARC data. In addition, with some simplifying assumptions, the self-heat rate and pressure rise rate data obtained during the low ϕ factor tests can be used in simple scale-up equations to size the emergency relief device.

To achieve a ϕ factor of ≈ 1.05, VSP [5] employs a light-weight test cell and a pressure equilibration system to accommodate the test cell's low pressure rating of ≈ 40 psi. However, the heater design of the VSP is crude and no calibration similar to ARC or APTAC is employed. As a result, VSP can experience various heat losses [6, 7] (< -0.15 °C/min) and heat gains [6, 7] ($> +0.05$ °C/min) as the sample temperature and pressure vary during testing. This limits VSP to an exotherm detection sensitivity of ≈ 0.2 °C/min. Since the ARC is ten times more sensitive than the VSP, the detected exotherm onset temperature by VSP is roughly 20 °C hotter than that detected by ARC and can be estimated for a simple *n*th-order reaction [7]. In addition, reproducibility of the VSP data is not as good as the ARC data.

Primarily because the VSP's exotherm detection sensitivity is only ≈ 0.2 °C/min, enhanced apparatuses, such as Union Carbide's APTAC and Hazard Evaluation Laboratory's PHI-TEC [8], were developed to achieve better exotherm detection sensitivity while using a light-weight test cell to achieve a ϕ factor close to 1. Following similar ideas and incorporating some of the features in APTAC, an enhanced adiabatic calorimeter (EAC) has been developed which allows both the exotherm onset temperature and direct scale-up data for emergency vent sizing to be obtained simultaneously. Characterizations of the EAC and a brief description are discussed below.

2. Experimental

2.1. Apparatus

A schematic illustration of the EAC device is shown in Fig. 1. The test cell, heaters, and magnetic agitation are located inside a high-pressure containment vessel. One of the main advantages over VSP is the use of three separate heating zones with PID control to achieve better temperature control and reduce temperature

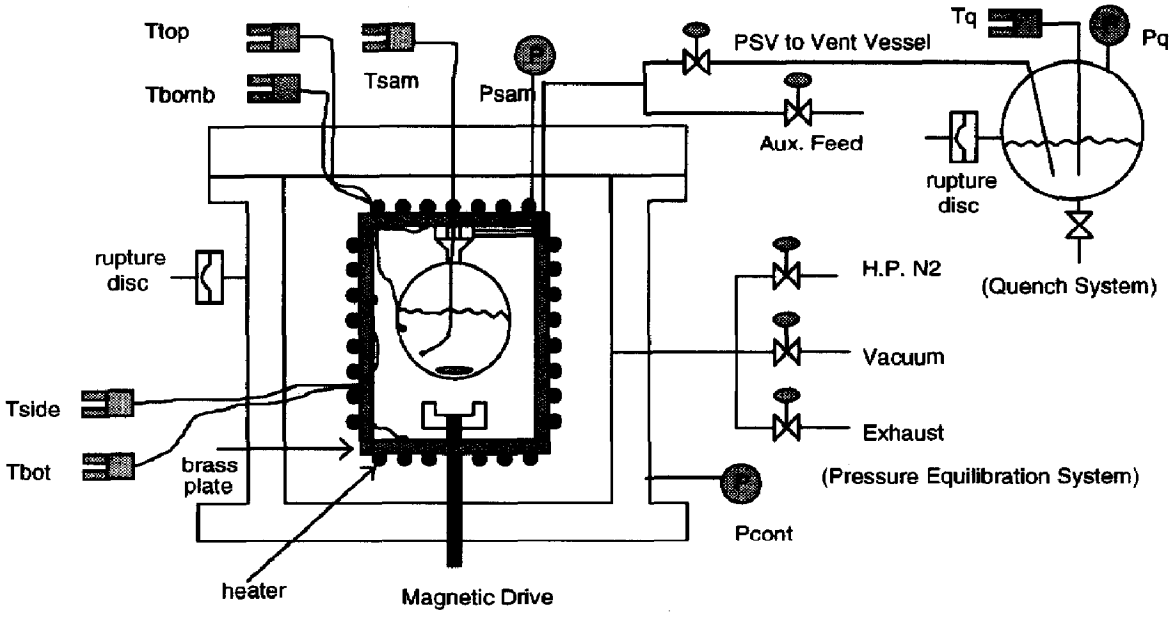

Fig. 1. Schematic illustration of EAC.

variations along the heater surface. All the heaters are 1/8″ brass plate with 1/8″ heating coils equally spaced and welded to the brass plate. The diameters of the top and bottom brass plates are 3.75″ and the inside diameter and height of the side plate are 3.5″ and 5.5″, respectively. The temperature variations along the surface of the top and bottom plates were found to be small; however, temperature variations up to $\approx 10\,^{\circ}C$ were observed for the side plate. As a result, to obtain smaller temperature variations for the side plate, brass should be replaced by copper in the future. The peak heater power output is $\approx 1.1\,kW$ for the top/bottom heater and $\approx 4.4\,kW$ for the side heater. At full power, the maximum temperature rise rates for the heaters are estimated to be $\approx 500\,^{\circ}C/min$.

The temperature measurements are made through type N thermocouples [9] since their signal reproducibility is better than type K thermocouples. In addition, similar to the ARC and APTAC [17], temperature calibration curves are employed to compensate for the heat loss or gain from the sample to the outside environment. The heat loss or gain is caused by many factors, such as mismatch of the thermocouples and the open space not covered by the heaters. During test runs, the temperatures of three heating zones are controlled to be equal to the sum of the sample temperature and a calculated calibration offset. Depending on the heater temperature and the containment vessel pressure, the calibration offset typically varies between $0\,^{\circ}C$ and $2\,^{\circ}C$. An attempt is being made to minimize the dependence of calibration on pressures. Furthermore, either an auxiliary heater or software heating is used to heat the test material to the desired holding temperatures or to simulate an external fire scenario. The software heating can be achieved by maintaining a constant positive

temperature difference between the heater temperature and the sum of the sample temperature and the calibration offset.

Similar to the APTAC, typical EAC test cells are 2.5″ ID, spheres with a 1″ long neck made of 3/8″ tubing. The weight of EAC spheres ranging from ≈ 30 to ≈ 75 g is slightly heavier than the typical VSP test cell weight of ≈ 30 to ≈ 50 g. As a result, the ϕ factor is either the same or slightly larger. Depending on the material of construction, pressure ratings for the 2.5″ spheres at a pre-set maximum operating temperature of 400 °C vary from ≈ 350 to ≈ 650 psi. To achieve a desirable maximum operating pressure of ≈ 1200 psig, a pressure equilibration system similar to VSP is used to maintain a pressure differential between the test cell and containment vessel less than the pressure rating of the test cell. In addition, if the test cell pressure exceeds the pre-set maximum operating pressure, the test is automatically terminated by shutting off the heaters and opening a safety relief valve to discharge the excess pressure.

Due to the flexibility in its design, EAC can use spheres of variable diameter, up to 2.5″ as test cells. EAC can be employed to simulate typical ARC runs if a 1″ ID sphere is used as a test cell and tests conducted under this mode have been compared with ARC data [10]. Since the pressure rating of typical 1″ test cells is much greater than ≈ 1200 psi at ≈ 400 °C, a pressure equilibrium system is not needed for this application.

The test cell is attached to a 3/8″ to 1/16″ reducing union with two additional 1/16″ male swagelok connections welded on the side. The pressure transducer is connected to one of the side 1/16″ port to monitor the pressure during testing. The other 1/16″ port allows sample introduction during testing. This line is also connected to a pressure relief valve which can be activated to relieve the pressure if the pressure exceeds ≈ 1200 psig. Downstream of the pressure relief valve, a 0.5 l vessel partially filled with compatible quench fluid, is employed to catch and quench the discharge from the test cell. This vessel has a pressure rating of ≈ 1000 psig and is protected by a rupture disk rated for 1000 psig.

Agitation of the test sample is achieved by using magnetic stirring. A small sample magnet is placed inside the test cell and driven by a strong horseshoe magnet, which sits underneath the test cell and is rotated by a magnetic drive designed to withstand high pressure. The distance between the sample bomb and horseshoe magnet is ≈ 1/4″ to achieve sufficient magnetic coupling.

2.2. *Instrumentation*

A schematic illustration of the instrumentation used to perform the tasks of data acquisition and control is shown in Fig. 2. The signals from three pressure transducers and the agitation speed are converted into 0–5 V DC signals and connected to a 16-bit PC A/D board through a multiplexer. All the thermocouple signals are connected to the same signal amplifier through a multiplexer to minimize the uncertainty from using multiple amplifiers. These two multiplexers are used to reduce cost and to provide simple means of adding more temperature and pressure inputs. However, the use of multiplexers has limited the maximum data

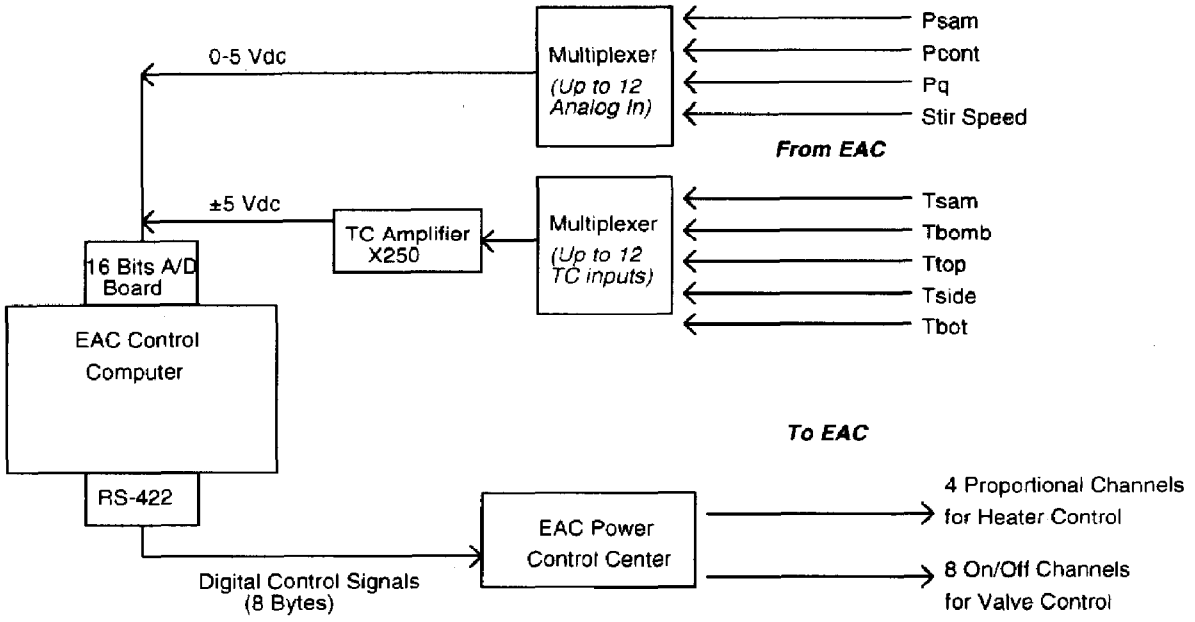

Fig. 2. Schematic illustration of the EAC data acquisition and control system.

acquisition rate to ≈ 30 points/s, which is still adequate for following a fast exotherm. The 16-bit A/D board is used to provide better signal resolution versus the popular 12-bit board. For temperature readings, the signal resolution is ≈ 0.01 °C versus ≈ 0.16 °C for a typical 12-bit board.

The control of heaters and valves is achieved through a custom-made power control center. The power center receives a digital control signal from the operating personal computer through a serial RS-422 line. The first byte of the control signal is used to notify the power center for incoming control data. The next four bytes provide a value between 0 and 200 as a proportional signal for the corresponding heaters. In every time 2 s interval, the power supplied to the heater for a fraction of time is equivalent to the control signal divided by 200. Every bit in the sixth byte of the control signal indicates the on/off status of the corresponding valves or switches. The last two bytes provide termination and error checking functions. In addition, the power center switches off all power if the heater temperature exceeds a high-temperature limit of 500 °C.

In-house software has been developed for the control computer to operate the EAC, collect data, and perform all the necessary functions. An averaging and regression strategy is employed in this software to address problems associated with the noises in temperature and pressure measurements. The temperature and pressure signals before amplification are in mv range and easily affected by the electrical powers and magnetic drive located close-by. In the software strategy, the number of readings used for averaging is determined as a function of the temperature and pressure rise rates. These readings are divided into 20 groups and the averages for each group are calculated. Regression is then performed

using these 20 average values to obtain the temperature and pressure rise rates. In addition to the calculated temperature and pressure rise rates, the stored data point also contains the calculated time, temperature, and pressure in the latest average values of these 20 average points. This strategy has been checked with computer simulation by using simple *n*th-order reaction models. In addition, the same strategy was shown to collect data which are comparable with the data collected by the ARC's processor [11].

3. Nonreactive system test

3.1. Effect of calibration uncertainty on drift rate

For EAC, the typical sample temperature is from ambient temperatures to $\approx 400\,^{\circ}C$ and the sample pressure is from vacuum to ≈ 1200 psig. The temperature and pressure exhibited by the sample during testing cause the corresponding changes of these two parameters in the space between the heaters and test cell. Inside the heating zone, the temperature varies from ambient temperature to $\approx 400\,^{\circ}C$ and the pressure varies from vacuum to ≈ 800 psig. Effects of these variations have been studied to characterize the precision of EAC.

Figure 3 displays the effect of temperature and chamber pressure on the measured instrument drift (°C/min) by assuming the calibration values deviate from the precise ones by 0.1 °C. With EAC, typical uncertainty in calibration value is within $\pm 0.1\,^{\circ}C$. As shown in Fig. 3, the drift rate increases with the temperature and pressure. The increase in temperature promotes radiation heat transfer and the increase in pressure promotes convection heat transfer. Because of these two effects, and consistent with observations in other commercial apparatuses such as ARC and VSP, EACs performance is expected to decrease as the heat transfer (i.e. the temperature and pressure) outside the test cell increases.

At all temperature levels, the drift rate decreases as the chamber pressure decreases. Therefore, to achieve the best possible performance, the chamber pressure is normally maintained under vacuum or the difference between sample pressure and test cell pressure rating, whichever is larger. In this manner, the effect of calibration uncertainty can be minimized to achieve an absolute drift rate much less than the target exotherm detection sensitivity of $\approx 0.02\,^{\circ}C$/min. Since the typical sample pressure at the initial stage of an exotherm is usually low, the detected exotherm onset temperature can then be measured with the least uncertainty.

3.2. Adiabatic aging test by using toluene

To detect the exotherm onset temperature at a rate much less than the detection sensitivity of an adiabatic calorimeter, the adiabatic aging test, which maintains the sample under adiabatic conditions over an extended period of time, is frequently used.

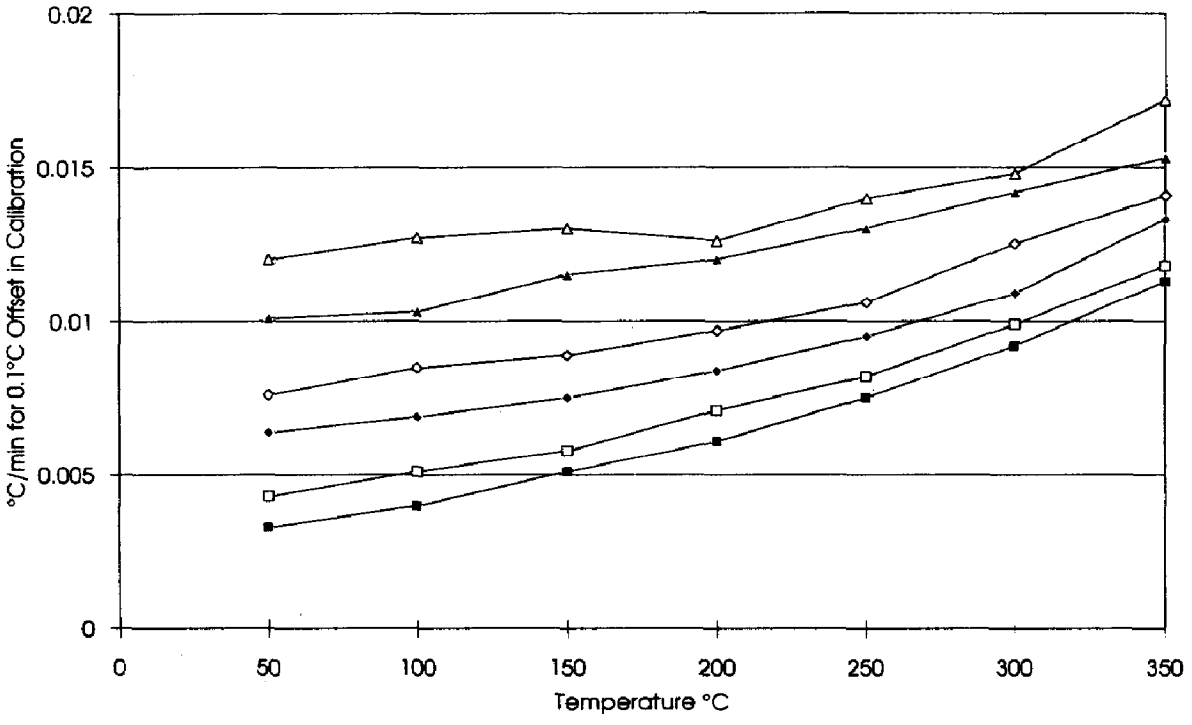

Fig. 3. Effect of temperature and chamber pressure on drift rate. Test system: 50 ml of Dowtherm A in a 48 g stainless steel test cell. (■) -12 ± 2 psig; (□) 0 ± 2 psig; (◆) 50 ± 2 psig; (◇) 100 ± 2 psig; (▲) 200 ± 2 psig; (△) 300 ± 2 psig.

This test mode is similar to the isothermal aging test mode employed during the Differential Scanning Calorimeter (DSC) testing.

If a nonreative sample, such as toluene, is employed during the adiabatic aging test, the measured average temperature increase/decrease rate is also referred as the drift rate [6]. For ideal performance simulating perfect adiabatic conditions, the measured drift rate plus its standard deviation, which characterize the accuracy and reproducibility of the test results, should be very close to 0.00 °C/min.

The measured drift rates for VSP, ARC, and EAC are listed in Table 1. For VSP, the drift rate was found to be positive in the relatively low temperature and pressure region and negative in the high temperature and pressure region [6, 7]. In addition, the standard deviation of the drift rate increases with the temperature and pressure. The combined effects of the drift rate and its standard deviation have limited VSP to an exotherm detection sensitivity of ≈ 0.2 °C/min. One of the main causes for the VSP's relative poor performance is that the VSP does not employ calibration curves to compensate the heat loss/gain observed while matching sample and jacket thermocouple readings.

In contrast to the VSP, the EAC demonstrated a significantly reduced drift rate and standard deviation, always lower than ± 0.01 °C/min at various temperatures

Table 1
Adiabatic drift rate (°C/min) by using toluene

Instrument[a]	120 °C (≈ 15 psig)	200 °C (≈ 100 psig)	300 °C (≈ 460 psig)
VSP (Round Robin, 9 runs) [6]	+ 0.03 (± 0.09)	− 0.12 (± 0.13)	Not tested
VSP (Project Manual) [7]	> 0.05	> 0.05	− 0.04
VSP (Merck, 6 runs)	+ 0.02 (± 0.04)	+ 0.05 (± 0.09)	Not tested
EAC (Merck, 3 runs)	− 0.007 (± 0.005)	− 0.000 (± 0.008)	+ 0.004 (± 0.008)
ARC (Tou et al.) [3]	− 0.002	+ 0.001	+ 0.003

[a] For the VSP, the insulation procedures employed from various sources are probably different and the data from project manual and Merck are obtained after recent in-house modifications. In EAC, a constant chamber pressure of 100 ± 2 psig was employed. The ARC's adiabatic drift data were obtained by using an empty test cell.

while under a chamber pressure of ≈ 100 psig. With these improvements, EAC has achieved an exotherm detection sensitivity of ≈ 0.02 °C/min (≈ 0.5 w/kg), which is similar to that of ARC. In addition, similar to ARC, if adiabatic aging tests are desired, thorough calibration may be conducted in the temperature region of interest to obtain more precise calibration may be conducted in the temperature region of interest to obtain more precise calibration values. In this manner, the drift rate for EAC may be less than ≈ 0.002 °C/min (≈ 0.05 w/kg) to achieve enhanced exotherm detection sensitivity.

4. Reactive system test

To further validate the performance of EAC, a known reactive system was tested. Characteristics of the measured exotherm can then be used for evaluation purposes, and the results compared to accepted values. Important parameters obtained or derived from the test data are the detected exotherm onset temperature, the heat of reaction (or the adiabatic temperature rise), the activation energy, the reaction order, and the pre-exponential factor. Several reactive systems have been studied extensively in both VSP and ARC. For this evaluation, a ≈ 15 wt% DTBP in toluene solution was utilized since extensive data on both ARC [3] and VSP [6] have been published. This decomposition reaction is known to be first order. Table 2 summarizes the testing results obtained from the EAC and Table 3 lists the results from various sources.

Based on the activation energy and pre-exponential factor listed in Table 3, first-order rate constants as a function of temperatures are plotted in Fig. 4. The curve based on the EAC data is bounded between the ARC data on the high side and the isothermal gas-phase decomposition data [16] on the low side. Results from VSP, EAC, and two half-life studies [12, 13] are in close agreement with

Table 2
Summary of EAC test data on DTBP in toluene

Bomb type	Conc. (wt%)	ϕ[a]	T_{onset} (°C)	dT/dt_{onset} (°C/min)	T_{max} (°C)	dT/dt_{max} (°C/min)	T_{end} (°C)	ΔT_{adia} (°C)	ΔH_r (kcal/mol)	E_{act} (kcal/mol)	log A (s^{-1})	n_g/n_{DTBP}[b]
Titanium	15	1.15	115.2	0.028	188.8	7.8	197.2	82	47.0	37.43	15.80	0.48
Hastelloy C	25	1.32	110.1	0.033	230.9	207	239.0	128.9	50.6	37.30	15.73	0.61
Stainless steel	20	1.16	114.8	0.031	215.3	65.8	225.0	110.2	47.6	37.28	15.70	0.50
Stainless steel	≈ 18[c]	1.16	132.9	0.25	222.2	123.6	233.0	100.1	—	37.29	15.71	0.51
Average									48.4 (± 1.9)	37.33 (± 0.07)	15.74 (± 0.05)	0.53 (± 0.06)

[a] The average heat capacities used for titanium, hastelloy C, stainless steel, DTBP, and toluene are 0.13, 0.1, 0.1, 0.5, and 0.5 cal/g°C, respectively.
[b] This term represents the molar ratio of the overall gas generation versus the initial DTBP charge.
[c] In this test, the initial concentration of DTBP before exotherm was not accurately determined and the test accidentally started at ≈ 132.9 °C. Since the first-order kinetic analysis is independent of the initial concentration, this set of data is still used to estimate activation energy and pre-exponential factor.

Table 3
Summary of kinetics information derived from DTBP studies

Instrument[a]	E_A (kcal/mol)	$\log_{10} A$ (s^{-1})	ΔH_r (kcal/mol)	T_{onset}
VSP (Round-Robin, 16 runs) [6]	36.1 (± 1.0)	15.13 (± 0.47)	49 (± 3)	130 °C
EAC (Merck, 4 runs)	37.33 (± 0.07)	15.74 (± 0.05)	48.4 (± 1.9)	115 °C
ARC (Tou et al.) [3]	37.80 (± 1.1)	16.15 (± 0.61)	43 (± 3.5)	117 °C
Shaw et al. [16]	37.78 (± 0.06)	15.8 (± 0.07)	Not available	Not available

[a] The heat of reaction for the VSP round robin tests was roughly estimated from the reported adiabatic temperature rise. The detected exotherm onset temperature (T_{onset}) for ARC is measured from 20 wt% DTBP in toluene solution.

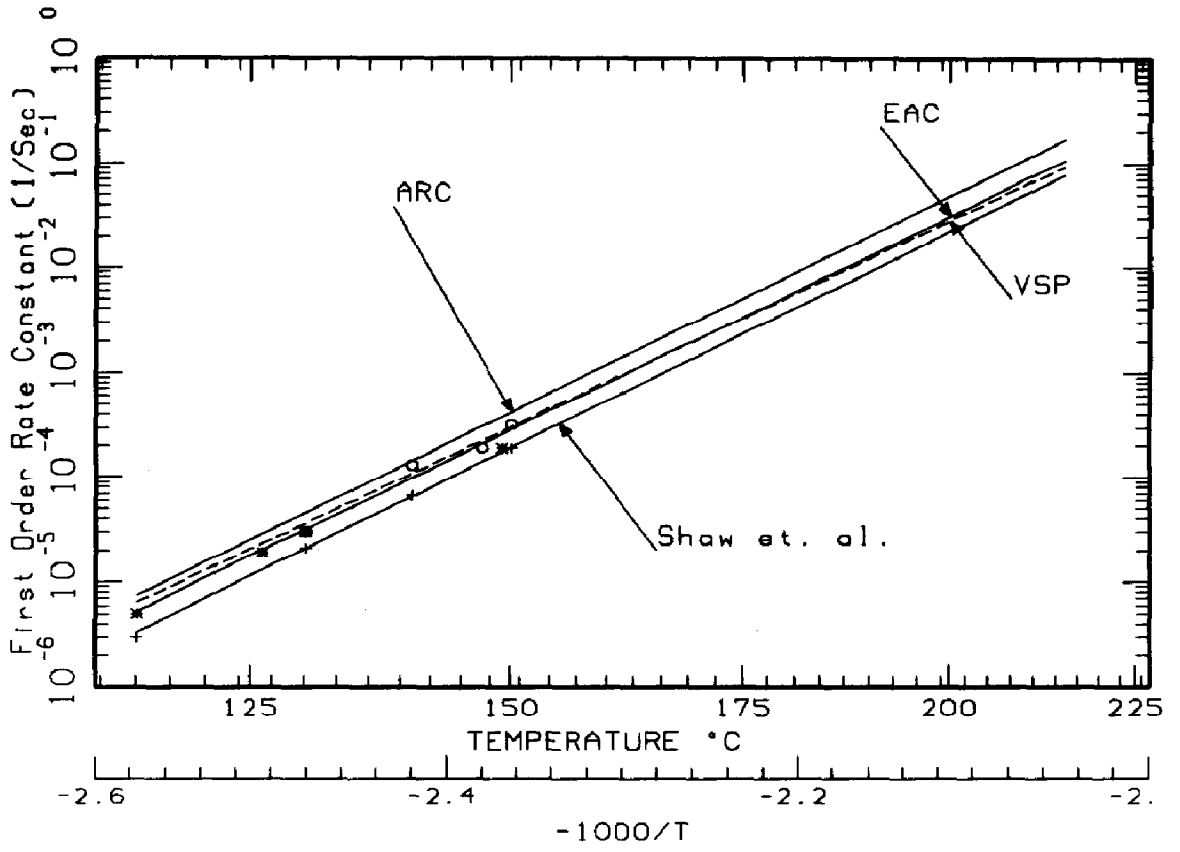

Fig. 4. First-order rate constant for DTBP decomposition. Half-life studies: (○) 5% DTBP in hydrocarbon [13]; (*) 0.2 M DTBP in benzene [12]; (+) DTBP in *n*-decene [12].

each other. The slight difference between VSP and EAC is probably due to that VSP tends to show positive drift at relatively low temperature and pressure and negative drift at high temperature and pressure.

The heat of reaction estimated from both VSP and EAC are also in close agreement. For ARC, the heat of reaction is about 13% lower than predicted from VSP data. This difference agrees with findings of others [10, 14, 15] that, in testing an energetic system such as DTBP, the heat of reaction estimated from standard ARC runs is typically 10–20% lower than that obtained from VSP. The primary cause for this difference is the lack of direct sample temperature measurement in the ARC's standard testing mode.

The detected exotherm onset temperature for 15 wt% DTBP in toluene from the EAC or ARC is much lower than that from the VSP. This is primarily due to the difference in the exotherm detection sensitivity. Under identical detection sensitivity as the ARC and at a lower ϕ factor, the observed exotherm onset temperature from EAC, as expected, is slightly lower than that from the ARC.

5. Discussion

An EAC has been designed and constructed which possesses a low ϕ factor and an enhanced exotherm detection sensitivity of $\approx 0.02\,^{\circ}\mathrm{C/min}$. This represents a significant improvement over the VSP. Owing to EAC's improved performance, it may be used to replace the closed VSP tests. Data obtained from the EAC may also be utilized to simulate process upset scenarios, characterize runaway reactions, and estimate vent sizes by applying DIERS technology.

Typical sample size of the EAC is ≈ 16 times larger than that of standard ARC experiments. The larger sample size reduces the effects of some unavoidable interferences during testing, such as the effect of fittings, reflux cooling in tubing located outside the heating zones, and the thermal lag during a fast exotherm. Additionally, the larger sample sizes translates into smaller ϕ factors, thus implying that the detected exotherm onset temperature with the EAC will be lower than that from the ARC. A simple equation can be used to estimate this difference for nth-order reactions when the exotherm detection sensitivities equal [7].

$$\frac{1}{T_{i,\mathrm{EAC}}} - \frac{1}{T_{i,\mathrm{ARC}}} = \frac{R}{E_{\mathrm{A}}} \ln\left(\frac{\phi_{\mathrm{ARC}}}{\phi_{\mathrm{EAC}}}\right),$$

where $T_{i,\mathrm{EAC}}$ and $T_{i,\mathrm{ARC}}$ are the measured exotherm onset temperatures from the ARC and the EAC, respectively, R is the gas constant, E_{A} is the activation energy, ϕ_{ARC} and ϕ_{EAC} are the experimental ϕ factor during ARC and EAC experiments, respectively. For the example reactive system consisting of ≈ 15 wt% DTBP in toluene, the difference in detected exotherm onset temperature is found to be

$$(T_{i,\mathrm{ARC}} - T_{i,\mathrm{EAC}}) \approx 4\,^{\circ}\mathrm{C},$$

which is close to the $\approx 2\,^{\circ}\mathrm{C}$ difference observed experimentally. However, the larger sample size employed in the EAC creates increased safety concerns during testing due to the increased energetic potential.

The EAC may be extended to approximate the open VSP test, which allows the test samples to evaporate to a much larger and cooler containment vessel. The open VSP tests are typically conducted for highly energetic materials or materials that would exhibit pressure greater than $\approx$ 1500 psi in a closed test. In the open VSP test, the chemical vapors may attack the interiors of VSP containment vessel and sometimes cause instrument malfunction. As a result, instead of direct simulation of the open VSP test, an alternative EAC test mode which simulates actual relief venting is under investigation.

6. Final remark

Since the EAC was validated, it has been substituted in $\approx$ 60% of VSP testing load. Since the EAC has significantly improved performances versus the VSP and the test set-up time is also greatly reduced, its usage will be increased as operational experience accumulates.

Acknowledgement

The author would like to express his sincere gratitude to S. Chippet and M. Young of Union Carbide Corp. for their suggestions and to K. Carlson, P. Lee, A. Price, J. Sharkey, and other members of Merck's Process Safety Laboratory for their ideas and assistance during the construction of EAC.

References

[1] H.G. Fisher et al., Emergency Relief System Design Using DIERS Technology, AIChE, New York, 1992.
[2] S. Chippet, VSP wish list, October 3, 1989, 6th DIERS Users Group Meeting.
[3] J.C. Tou and L.F. Whiting, The thermokinetic performance of an accelerating rate calorimeter, Thermochimica Acta, 48 (1981) 21–42.
[4] D.I. Townsend and J.C. Tou, Thermochimica Acta, 37 (1980) 1.
[5] J. Leung, M.J. Creed and H.G. Fisher, Thermal runaway reactions in a low thermal inertia apparatus, Thermochimica Acta, 104 (1986) 13–29.
[6] J. Leung, M.J. Creed and H.G. Fisher, Round Robin vent sizing package results, Int. Symp. on Runaway Reactions, 1989.
[7] J.A. Noronha and H.G. Fisher, Emergency Relief System Design Using DIERS Technology, AIChE, New York, Chap. VI, 1992, pp. 386–387.
[8] J. Singh, PHI-TEC: enhanced vent sizing calorimeter – application and comparison with existing devices, Int. Symp. of Runaway Reactions, 1989, pp. 313–330.
[9] N.A. Burley, Nicrosil/Nisil type N thermocouple, Measurements and Control (1989).
[10] M. Yue, Limitations of ARC's standard testing mode in runaway kinetics study: discussion based on BPO testing, DIERS Users Group Meeting, May 1992.
[11] M. Yue, An independent data acquisition system for ARC, First Ann. Northeast ARC Users Group Symp., October 1991.
[12] Lucidol Technical Data, Evaluation of organic peroxides from half-life data, bulletin 30.30, 1986.

[13] L.A. Medard, Accidental Explosions Vol. 2: Types of Explosive Substances, Wiley, New York, Chap. 21, 1989, pp. 489–491.
[14] A. Chakrabarti, Unique application of VSP, 11th DIERS Users Group Meeting, May 1992.
[15] J. Leung, Phase V round-robin final data presentation, 11th DIERS Users Group Meeting, May 1992.
[16] D.H. Shaw and H.O. Pritchard, Thermal decomposition of di-tert-butyl peroxide at high pressure, Can. J. Chem., 46 (1968) 2721–2724.
[17] S. Chippet and M. Young et al., private communication, 1991.